



Research on a simulated 60 kW PEMFC cogeneration system for domestic application*

ZHANG Ying-ying (张颖颖), YU Qing-chun (余晴春), CAO Guang-yi (曹广益), ZHU Xin-jian (朱新坚)

(Fuel Cell Institute, Shanghai Jiao Tong University, Shanghai 200030, China)

†E-mail: tricia@sjtu.edu.cn

Received Apr. 4, 2005; revision accepted Oct. 11, 2005

Abstract: The electrical and thermal performances of a simulated 60 kW Proton Exchange Membrane Fuel Cell (PEMFC) cogeneration system are first analyzed and then strategies to make the system operation stable and efficient are developed. The system configuration is described first, and then the power response and coordination strategy are presented on the basis of the electricity model. Two different thermal models are used to estimate the thermal performance of this cogeneration system, and heat management is discussed. Based on these system designs, the 60 kW PEMFC cogeneration system is analyzed in detail. The analysis results will be useful for further study and development of the system.

Key words: Proton Exchange Membrane Fuel Cell (PEMFC), Cogeneration, Coordination strategy, Power response, Heat management

doi:10.1631/jzus.2006.A0450

Document code: A

CLC number: TM911.4

INTRODUCTION

Distributed cogeneration technology is a hot topic in electrical and energy industries (Ferguson and Ugursal, 2004). China's need to limit the power usage in some places to meet the peak power demand in summer of recent years stimulated and supported increasing research on distributed generation technologies. Fuel cells, as renewable energy sources, are considered one of the most promising sources of distributed electrical power. Operational fuel cell systems have performance superior to that of 5 kW to 2 MW combustion-based generators supplying the electrical requirements of most buildings. Fuel cells produce surplus heat suitable for heating small buildings. Much attention have been focused on PEMFC, whose waste heat has potential use for small-scale buildings.

The electrical and thermal demands of residences are high and vary greatly in different time, seasons,

and occupancy patterns. So PEMFC cogeneration system must manage heat to achieve as high as possible efficiency in response to electrical demand. It is very important that the PEMFC cogeneration system is designed effectively on the basis of detailed analysis. How to meet the electrical demand. How much heat can be recovered and how to manage and use it. What is the total efficiency of the system. These results are useful for the design and development of PEMFC cogeneration system.

The 60 kW PEMFC cogeneration system researched in this work supplies 15 residences. For better performances and the security, stability and durability, the parameters coordination, the load power response and the heat management of the system are all important and so, are carefully considered. The system configuration and operation requirements are described first. Then a generalized model is established and validated on the basis of the electricity model. The control oriented system dynamics models of Pukrushpan *et al.* (2004) are used to establish the coordination and power response strategy proposed and tested. Two different thermal

* Project (No. 2002AA517020) supported by the Hi-Tech Research and Development Program (863) of China

models in literature are used to estimate the system thermal performance, and heat management is discussed. At last, simulation tests present results of study on the electrical and thermal supplies of the system in typical summer and winter days. Some system application problems are analyzed. This is the comprehensive research on the cogeneration system. The system tests results supply useful information for further development and research.

SYSTEM OVERVIEW

The 60 kW PEMFC cogeneration system designed is shown in Fig.1. The PEMFC stack is comprised of 300 series-connected cells with total active area of 600 cm². Nafion membrane with thickness of 0.0175 cm is used. A compressor is needed to compress air to the desired pressure level. Filtered, cooled and humidified air is supplied to the cathode. An exit valve controls the air exit flow rate, allowing exit of some vapor from the cathode. The pressure of the pressurized hydrogen supplied from a container reduced to 0.6 MPa. The second valve adjusts the hydrogen flow rate. A humidifier is used to humidify the hydrogen flow. Ferguson *et al.*(2003) reported that the PEMFC system performance is sensitive to the temperature, and may deteriorate by as much as 60% with deviations of 15 °C from the design operating temperature. The excess heat is recovered from the PEMFC system by the cooling water. As shown in Fig.1, a hot water tank stores the recovered heat and uses it for cooling circulation and supplying heat for houses. The gas burner and safety valve added to the hot water tank can be turned on or off as required to maintain the temperature within the ideal range.

The system must have satisfactory heat and power performance and characteristics of security, stability and durability. From experiences on PEMFC above kW level system, we decided that 60 kW PEMFC cogeneration system operating at 75 °C. In this system, cathode pressure is maintained at 0.3 MPa and anode pressure is lower by 0.01 MPa than cathode pressure, and anode and cathode humidity are both kept at 100%. The oxygen excess ratio is set to 2.

PEMFC SYSTEM ELECTRICITY MODEL

Electricity model

The cell voltage model was studied empirically and physically by many researchers. For control design, the model must be simple and reasonable. So, in this study, a generalized electrical model of PEMFC is developed by using a combination of physical and empirical modelling techniques based on GSSEM developed by Amplett *et al.*(1995a; 1995b). Water transport across Nafion membrane was studied by Dutta *et al.*(2001), who found that

$$P_{st} = nV_{fc} I_{st} = nI_{st} (E - \eta_{act} - \eta_{ohmic}), \quad (1)$$

$$E = E^0 + 4.308 \times 10^{-5} T_{st} [\ln(p_{H_2,an} / 101325) + \ln(p_{O_2,ca} / 101325) / 2], \quad (2)$$

$$E^0 = 1.53 - 2.04 \times 10^{-3} T_{st} + 3.1 \times 10^{-9} T_{st}^2 + 6.06 \times 10^{-13} T_{st}^3 + 1.78 \times 10^{-4} T_{st} \ln(T_{st}), \quad (3)$$

$$\eta_{act} = \xi_1 + \xi_2 T_{st} \ln(c_{O_2}) + \xi_3 T_{st} \ln(A) + \xi_4 T_{st} \ln(c_{H_2}) + \xi_5 T_{st} \ln(I_{st}) + \xi_6 T_{st}, \quad (4)$$

$$c_{O_2} = \frac{p_{O_2,ca} / 101325}{5.08 \times 10^6 \exp(-498 / T_{st})}, \quad (5)$$

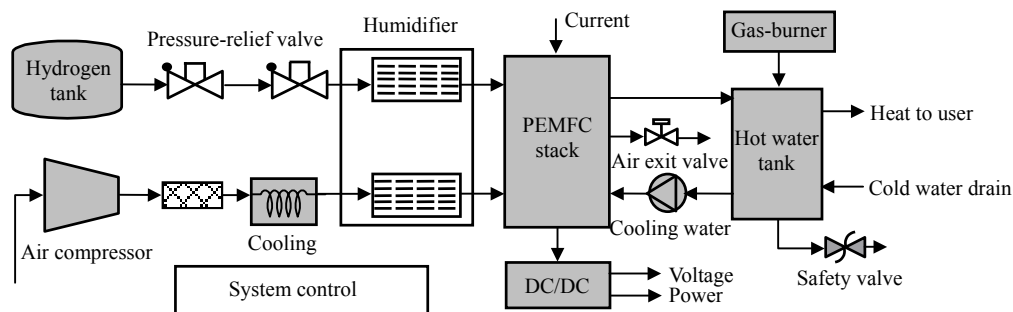


Fig.1 60 kW PEMFC cogeneration system block diagram

$$c_{H_2} = \frac{p_{H_2,an}/101325}{1.09 \times 10^6 \exp(77/T_{st})}, \quad (6)$$

$$\begin{aligned} \eta_{ohm} &= I_{st} t_{mem} / (A \sigma_{mem}), \\ \sigma_{mem} &= (0.00514 \lambda_{mem} - 0.00326) \\ &\quad \times \exp[1268(1/303 - 1/T_{st})], \end{aligned} \quad (7)$$

where P_{st} is the stack power, n is the cell number, V_{fc} is cell voltage, and I_{st} is cell current, E is the open circuit voltage, η_{act} is the activation overvoltage, η_{ohmic} is the ohmic overvoltage, T_{st} is the temperature, $p_{H_2,an}$ is the hydrogen reactant partial pressure, $p_{O_2,ca}$ is the oxygen reactant partial pressure, A is the active area, c_{H_2} and c_{O_2} are hydrogen and oxygen concentration at the anode and cathode respectively, t_{mem} is the membrane thickness, σ_{mem} is the membrane conductivity, λ_{mem} is the membrane water content, ξ_i are empirical coefficients for calculating activation overvoltage. According to Eqs.(1)~(7), the electricity model is applicable for PEMFC stack of various configurations and operating conditions.

In addition to a stack, there are many auxiliary components such as air compressor, humidification pumps and valves in the system, which consume the power generated by the system itself directly. Among them, the air compressor is responsible for up to 90% of total power loss. So, the net power of the system can be calculated simply as

$$P_{net} = P_{st} - P_{cp}, \quad (8)$$

where P_{cp} is the power loss of air compressor, which is proportional to the air flow rate. According to PEMFC, when ambient air is assumed to be ideal gas consisting of 21% molar portion of oxygen and 79% molar portion of nitrogen, the air supplied to the cathode is

$$N_{air} = \lambda_{air} \frac{nI_{st}}{0.21 \times 4F}, \quad (9)$$

where N_{air} is air molar flow, λ_{air} is air excess ratio, and F is the Faraday number. The hydrogen consumed in the stack is also described as a function of the stack current

$$N_{H_2} = nI_{st} / (2F). \quad (10)$$

So, only considering the electrical aspect of the system, the net efficiency is directly proportional to the net power supplied to the load, and inverse proportional to the fuel consumed:

$$\eta_{electr} = \frac{P_{net}}{N_{H_2} M_{H_2} HHV_{H_2}}, \quad (11)$$

where M_{H_2} is hydrogen molar mass, HHV_{H_2} is hydrogen higher heating value.

Model validation

Many electrical performance tests of PEMFC can be found in literature. Data from the Ballard Mark IV fuel cell have been extensively published (Amphlett *et al.*, 1995a; 1995b), based on which the parameters in the activation overvoltage model are obtainable by linear regression: $\xi_1 = -0.95159$, $\xi_2 = 7.3777 \times 10^{-5}$, $\xi_3 = 1.7332 \times 10^{-4}$, $\xi_4 = 4.3084 \times 10^{-5}$, $\xi_5 = -1.8627 \times 10^{-4}$, $\xi_6 = 0.003$. Fig.2 is the predicted electrical performance of the cell versus the experimentally measured performance. The model can accurately predict the performance of the cell over a fairly large range of voltages corresponding to current densities of as high as 1.0 A/cm². As mentioned before, the model is designed to be applied flexibly to a wide range of operation conditions and various configurations. So, it is validated by other tests results. Model predictions of output voltage vs published experimental data for a H₂/O₂ PEMFC using a Nafion115 membrane (Kim *et al.*, 1995) are shown in Fig.3. The model accurately predicts the voltage in the current density range of 0 to 1 A/cm². So the electricity model is correct and flexible, and can describe the PEMFC performance.

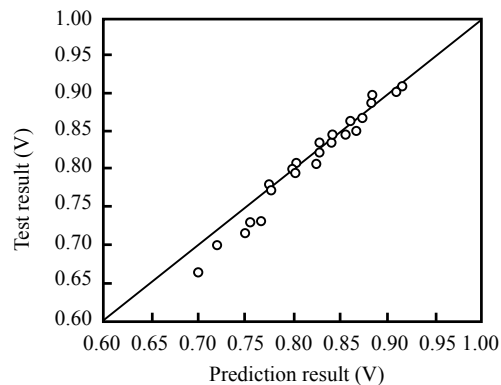


Fig.2 Predicted result of output voltage vs test result of Amphlett *et al.*(1995a; 1995b)

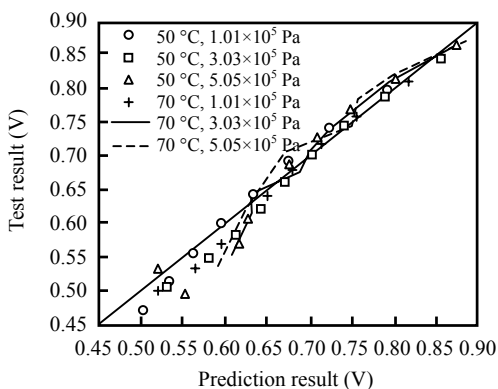


Fig.3 Predicted result of output voltage vs H_2/O_2 test result of Kim *et al.*(1995)

DESIGN FOR 60 kW PEMFC SYSTEM TO MEET ELECTRICAL DEMAND IN STEADY OPERATION

As said above, in order to achieve the good performance, security, stability and durability desired for the system, we decided to use the 60 kW PEMFC cogeneration system to meet the electrical demand under certain operating conditions. System coordination strategies are presented and tested. The air compressor is controlled to supply air at constant excess ratio of 2. Owing to the dynamic and nonlinear coupling between cathode pressure and humidity, the intelligent auto-adapted PI decoupling control method is used. A single neuron PI controller controls cathode humidity by adjusting the water injection to the cathode humidifier. Another similar controller adjusts the air exit valve to control cathode pressure. The quadratic index is introduced in order to realize optimal control. At the anode side, the humidity is controlled by adjusting the water injection and anode pressure is controlled by the pressure relief valve. These system control designs are realized in the simulated 60 kW PEMFC system, although there is only weak coupling between anode and cathode. Thus, under steady operation, parameters of $p_{H_2,an}$, $p_{O_2,ca}$,

λ_{mem} are all kept constant. It is assumed that the temperature T_{st} is also kept constant by the good cooling water circulation. Then, the relationship of the voltage, net power and current density of the stack can be described by certain polarization curves. Fig.4 is the experimentally measured polarization curve of 60 kW PEMFC system. Only if finding optimal

working points in curves in real-time, the system can meet the electrical demand. According to Hawkes and Leach (2005), typical electrical demand data at intervals of 10-min is appropriate to evaluate the performance of the domestic cogeneration system. So, a typical electrical demand of 15 houses is simulated for each 10-min of a day in summer based on the data in the final report for DOE NETL (2002). The system is tested to be able to meet it by optimally searching the working point in real-time, as shown in Fig.5.

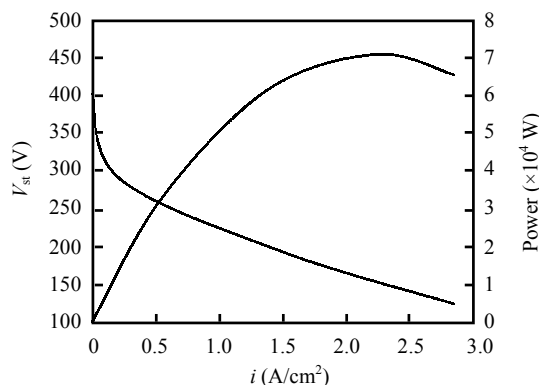


Fig.4 Polarization curve of the 60 kW PEMFC system in steady operation

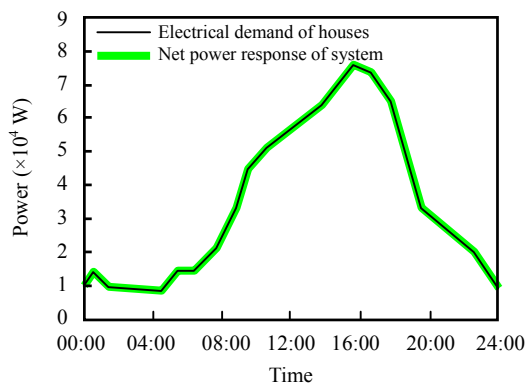


Fig.5 60 kW PEMFC system response to the electrical demand of houses in a day of summer

PEMFC SYSTEM THERMAL MODEL

The thermal model here is not for analyzing the internal heat diffusion process, but for giving some guidelines for the system heat management by estimating the heat produced, recovered, stored and supplied. As there is no full and accurate experi-

mental results, the accuracy of thermal performance predictions are assessed by comparing estimates of two different models. Furthermore, use of two models together help provide better analysis of thermal performance.

First thermal model

One model is based on the simplified thermal model of PEFC system presented by Ferguson and Ugursal (2004). It includes two control volumes. The electrochemical and thermal processes occurring on the gas side of the stack are modelled in the first volume and the cooling water side of the stack heat exchanger is represented in another volume. The reaction occurring in the PEMFC stack is $2\text{H}_2 + \text{O}_2 \rightarrow 2\text{H}_2\text{O}$. According to the Hess theory, the energy produced in the chemical reaction is quantified by the enthalpy change that occurs inside the stack:

$$\Delta H_{\text{st}} = (Nh)_{\text{H}_2} + (Nh)_{\text{O}_2} - (Nh)_{\text{H}_2\text{O}}, \quad (12)$$

where the enthalpy of each matter can be evaluated using a relation in the form of $h(T)$. The reactants and product are all at the stack temperature. Owing to the overall efficiency of the stack, the chemical energy released in the stack cannot be all converted to electric work P_{st} , but some is converted into heat Q_{st} . The heat must be extracted to ensure efficient operation. According to Ferguson, if a minimum temperature difference ΔT_{min} exists between the cooling water and the stack, all heat available will be recovered by the cooling water. Thus the maximum amount of heat that can be transferred to the cooling water is decided by the minimum temperature difference ΔT_{min} :

$$Q_{\text{max}} = N_{\text{cw}} C_p ((T_{\text{st}} - \Delta T_{\text{min}}) - T_{\text{cw,in}}), \quad (13)$$

where $T_{\text{cw,in}}$ is the temperature of cooling water entering the stack. So, the heat recovered by the cooling water is limited by Q_{max} . If the amount of heat available is more than the Q_{max} , the unrecovered surplus heat must be extracted using an auxiliary heat rejection system, i.e. $Q_{\text{extract}} = Q_{\text{st}} - Q_{\text{recovery}}$. The heat recovery by the cooling water is a process of heat exchange from the stack to the water. The temperature change lead by this exchange is as follows:

$$Q_{\text{recovery}} = N_{\text{cw}} C_p (T_{\text{cw,out}} - T_{\text{cw,in}}), \quad (14)$$

where $T_{\text{cw,out}}$ is the temperature of cooling water exiting the stack.

Second thermal model

The second model is modified from the thermal model of SOFC system presented by Ferguson *et al.* (2003). The model includes three control volumes. The electrochemical reaction occurs in the first volume. In a real PEMFC stack, the heat produced is transferred directly from the stack to the cooling water, just as described in the first model. But, in this second model, the heat is assumed to be transferred to the product of the electrochemical reaction, raising its temperature. The first volume energy balance is as follows:

$$(Nh)_{\text{H}_2} + (Nh)_{\text{O}_2} + \phi_{\text{chemical}} = (Nh)_{\text{H}_2\text{O,product}} + P_{\text{st}} + Q_{\text{loss}}, \quad (15)$$

where, the heat lost $Q_{\text{loss}} = 0$ in the adiabatic condition, is the same as that in the first model. ϕ_{chemical} represents the chemical energy supplied to the stack, and connected with the hydrogen entering the stack

$$\phi_{\text{chemical}} = N_{\text{H}_2} \times HHV_{\text{H}_2}. \quad (16)$$

It is assumed that reactants (H_2 , O_2) temperature is equal to the stack temperature, but the temperature of the product (H_2O) becomes higher than the stack temperature after absorbing the heat produced in the chemical reaction. In the second volume, the high temperature product is cooled to the stack temperature and the heat is transferred to the cooling water. Then the exhaust (H_2O) exits the stack carried by the excess air. The process of the heat transferred is as follows:

$$(Nh)_{\text{H}_2\text{O,product}} = (Nh)_{\text{H}_2\text{O,exhaust}} + Q_{\text{recovery}}, \quad (17)$$

Q_{recovery} is the heat transferred from the high temperature product to the cooling water. If the cooling water can recover all this heat, the energy balance can be kept and the stack can operate in the desired temperature. The third volume represents the water side of the heat exchanger. This energy balance is the same as that in the first model.

Model validation

In the study, the thermal energy is estimated for the 60 kW PEMFC system on the basis of two thermal models. The system was controlled to meet the electrical demand and operate in the steady conditions. The ΔT_{\min} in the first model is determined as 9 °C from experience. Fig.6a shows the heat recovery predictions by the two models when the cooling water inlet temperature is 55 °C and the flow rate is 555.56 mol/s. It can be seen that the models predictions agree very well. Thus, two models can be used together to predict the heat recovered. Then the heat-to-power ratio is in the range of one to two, which agrees with an actual PEMFC system.

HEAT MANAGEMENT SYSTEM ANALYSIS AND DESIGN

Fig.6b shows the heat recovery predictions when the cooling water inlet temperature is increased to 65 °C. Predictions by two models are different. Because of the minimum temperature difference, the heat recovered by the cooling water in the first model is certain to be limited. But two models predict the same amount of heat recovery for all operating points at which the amount of heat available in the fuel cell is equal to or less than the maximum heat recovered. Comparing the results in Figs.6a and 6b, for the same flow rate, if the cooling water entered the stack with too high temperature, it cannot recover all the heat that should be recovered. Figs.6b and 6c show that for the same temperature, the cooling water can recover more heat by increasing flow rate through the stack. So, the heat recovered depends on the temperature and flow rate of the cooling water. In an actual system, the flow rate of the pump used to circulate the cooling water has a certain limitation on the flow rate. If the temperature of the cooling water is too high, the stack cannot be cooled enough only by cooling water. Conversely, the heat stored is not sufficient for houses. In this research, the temperature of the cooling water entering the stack is decided within the range of 55 °C to 65 °C and the temperature of the cooling water is increased 10 °C through the stack from experience. A pump adjusts the flow rate of the cooling water entering the stack to ensure efficient system operation.

The temperature of the cooling water entering

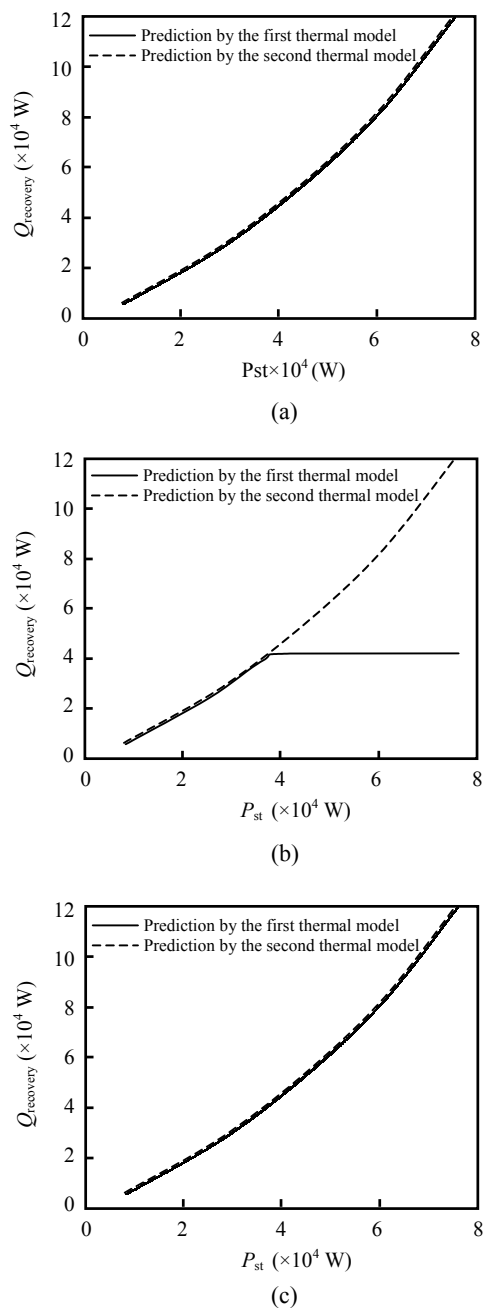


Fig.6 Heat estimations of two thermal models for the system in steady operation. (a) $T_{\text{cwi}}=55$ °C, $N_{\text{cw}}=555.56$ mol/s; (b) $T_{\text{cwi}}=65$ °C, $N_{\text{cw}}=555.56$ mol/s; (c) $T_{\text{cwi}}=65$ °C, $N_{\text{cw}}=2777.8$ mol/s

the stack is the same as that inside the hot water tank. So the temperature is an important parameter for the tank, which must be controlled within the desired range. High temperature water enters the tank, and low temperature cooling water exits. Some cool city water is added when supplying certain heat to houses.

And considering the heat loss from the high temperature tank to the environment, the temperature inside the tank is variable. To control the tank temperature, a gas burner and a safety valve are attached, which are turned on or off to maintain the tank temperature ideal, as presented by Ferguson *et al.*(2003) and Ferguson and Ugursal (2004). Certainly, the operation of the valve and the burner affect the total efficiency of the system. Thus, based on the thermal demand and the system performance, the tank should be designed to be able to not only store enough heat to meet the thermal demand but also make possible keeping the ideal temperature, without using other auxiliary components. In the research, the hot water tank is selected to be 1200 kg in mass, and the overall hot water tank heat loss coefficient is 15 W/°C.

SYSTEM APPLICATION PERFORMANCE ANALYSES

Sixty kW PEMFC cogeneration system operates in response to the electrical demand. The electrical and the thermal demands of family houses change independently and widely for the different time, seasons and occupancy patterns. Figs.7a and 7b show typical energy demands of fifteen family houses in days of summer and winter at intervals of 10-min (DOE NETL, 2002; Gunes, 2001). In summer, the electrical demand is far more than the thermal demand owing to large power required for electric refrigeration. The required heating load is only some hot water. But in winter, more hot water and space heating are required, so the thermal demand is much larger than the electrical one. For 60 kW PEMFC cogeneration system, the power response is the net output power. The heat available is the sum of the heat stored in the tank and the heat captured from the air cooler. The hot water separated from the exhaust air is used to humidify reactants. Figs.7a and 7b show the results of electrical and thermal supplies of the system. It can be seen that, in summer, the heat recovered is much more than houses required. But in winter, the heat recovered only approximates the hot water demand and much less than the space heating requirement. Though, the heat estimations based on models are all theoretical values, which are upper

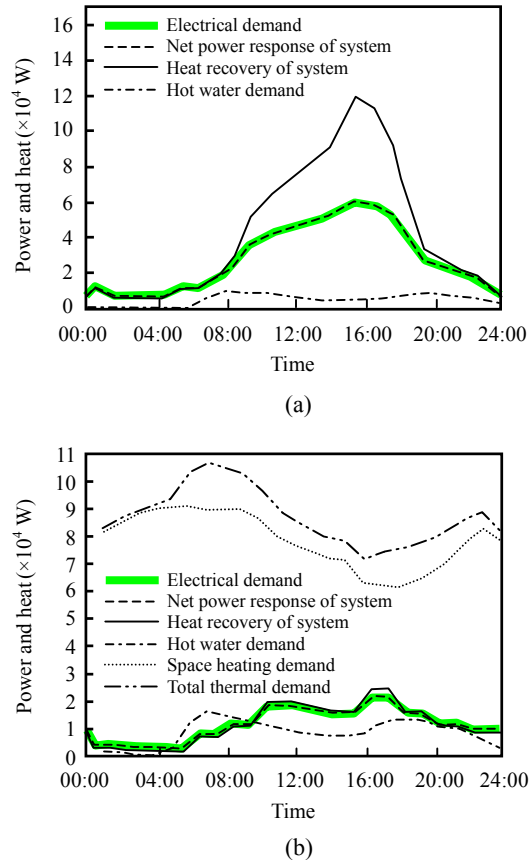


Fig.7 Energy demands and response of 60 kW PEMFC cogeneration system in a day of summer (a) and of winter (b)

range values essentially, they can help in evaluating the thermal behavior of the system. It is concluded that, in summer, some heat will be wasted. So, other thermal uses can be considered to decrease the waste of the heat and then increase the total efficiency of the system. In winter, the heat recovered is not enough to supply total thermal demand of houses. The hot water can be supplied by the system and the space heating requirement has to be met by other energy methods. Owing to the use of all energies, including the electrical and thermal energies, the cogeneration system has higher efficiency obviously. Therefore, the total efficiency of the system is also expressed in terms of the higher heating value of hydrogen:

$$\eta_{\text{system}} = \frac{P_{\text{net}} + Q_{\text{available}}}{N_{\text{H}_2} M_{\text{H}_2} \text{HHV}_{\text{H}_2}}, \quad (18)$$

where $Q_{\text{available}}$ is the heat available from the system.

In the test shown in Figs.7a and 7b, the average electrical efficiency is 0.4805 in winter and 0.4147 in summer. The total efficiency (combined thermal and electrical) is 0.8961 in winter and 0.9071 in summer, which are the maximum efficiencies in theory.

CONCLUSION

This work researches a 60 kW PEMFC cogeneration system for fifteen family houses. To study the system performance, a system model, mainly in electrical aspect, is established and validated. Based on it and some analyses, the steady operation and the electrical response are designed and realized. Then, two thermal models are used together to estimate the thermal performance. Some more detailed analyses and design of the heat management are presented. System simulation tests showed that the system responds to the power demand during real-time steady operation and supplies the hot water for houses as well. But, for better system performance, in the future, some improvements should be made in configuration designs and control strategies based on the current system results. And according to the system thermal performance in tests, other thermal utilizations should be researched to increase the system thermal efficiency. The results of this work provide some advice for system development and applications.

References

- Amphlett, J.C., Baumert, R.M., Harris, T.J., Mann, R.F., Peppley, B.A., Roberge, P.R., 1995a. Performance modeling of the Ballard Mark IV solid polymer electrolyte fuel cell I. Mechanistic model development. *J. Electrochem. Soc.*, **142**(1):1-8.
- Amphlett, J.C., Baumert, R.M., Harris, T.J., Mann, R.F., Peppley, B.A., Roberge, P.R., 1995b. Performance modeling of the Ballard Mark IV solid polymer electrolyte fuel cell II. Empirical model development. *J. Electrochem. Soc.*, **142**(1):9-15.
- DOE NETL (US Department of Energy, National Energy Technology Laboratory), 2002. Grid-independent, Residential Fuel-cell Conceptual Design and Cost Estimate. Final Report for DOE NETL in Subcontract to Parsons Infrastructure & Technology Group, Inc.
- Dutta, S., Shimpalee, S., van Zee, J.W., 2001. Numerical prediction of mass-exchange between cathode and anode channels in a PEM fuel cell. *International Journal of Heat and Mass Transfer*, **44**(11):2029-2042. [doi:10.1016/S0017-9310(00)00257-X]
- Ferguson, A., Ugursal, V.I., 2004. Fuel cell modeling for building cogeneration applications. *Journal of Power Sources*, **137**(1):30-42.
- Ferguson, A., Beausoleil-Morrison, I., Ugursal, V.I., 2003. A Comparative Assessment of Fuel Cell Cogeneration Heat Recovery Models. Proceedings of Building Simulation 2003, The Eighth International IBPSA Conference.
- Gunes, M.B., 2001. Investigation of a Fuel Cell Based Total Energy System for Residential Applications. Virginia Polytechnic Institute and State University.
- Hawkes, A., Leach, M., 2005. Impacts of temporal precision in optimisation modelling of micro-combined heat and power. *Energy*, **30**(10):1759-1779. [doi:10.1016/j.energy.2004.11.012]
- Kim, J., Lee, S., Srinivasan, S., Chamberlin, C.E., 1995. Modeling of proton exchange membrane fuel cell performance with an empirical equation. *J. Electrochem. Soc.*, **142**(8):2670-2674.
- Pukrushpan, J.T., Peng, H., Stefanopoulou, A.G., 2004. Control-oriented modeling and analysis for automotive fuel cell systems. *Journal of Dynamic Systems Measurement, and Control*, **126**(1):14-25. [doi:10.1115/1.1648308]